Diabetologia (2014) 57:950–959
DOI 10.1007/s00125-014-3166-3

ARTICLE

Non-invasive quantification of the beta cell mass by SPECT with ^{111}In-labelled exendin

Maarten Brom · Wietske Woliner-van der Weg · Lieke Joosten · Cathelijne Frielink · Thomas Bouckenooghe · Paul Rijken · Karolina Andralojc · Burkhard J. Göke · Marion de Jong · Decio L. Eizirik · Martin Béhé · Tony Lahoutte · Wim J. G. Oyen · Cees J. Tack · Marcel Janssen · Otto C. Boerman · Martin Gotthardt

Received: 7 November 2013 / Accepted: 23 December 2013 / Published online: 1 February 2014

Abstract
Aims/hypothesis A reliable method for in vivo quantification of pancreatic beta cell mass (BCM) could lead to further insight into the pathophysiology of diabetes. The glucagon-like peptide 1 receptor, abundantly expressed on beta cells, may be a suitable target for imaging. We investigated the potential of radiotracer imaging with the GLP-1 analogue exendin labelled with indium-111 for determination of BCM in vivo in a rodent model of beta cell loss and in patients with type 1 diabetes and healthy individuals.

Methods The targeting of ^{111}In-labelled exendin was examined in a rat model of alloxan-induced beta cell loss. Rats were injected with 15 MBq ^{111}In-labelled exendin and single photon emission computed tomography (SPECT) acquisition was performed 1 h post injection, followed by dissection, biodistribution and ex vivo autoradiography studies of pancreatic sections. BCM was determined by morphometric analysis after staining with an anti-insulin antibody. For clinical evaluation SPECT was acquired 4, 24 and 48 h after injection of 150 MBq ^{111}In-labelled exendin in five patients with type 1

Maarten Brom and Wietske Woliner-van der Weg contributed equally to this study.

Electronic supplementary material The online version of this article (doi:10.1007/s00125-014-3166-3) contains peer-reviewed but unedited supplementary material, which is available to authorised users.

M. Brom (✉) · W. Woliner-van der Weg · L. Joosten · C. Frielink · K. Andralojc · W. J. G. Oyen · M. Janssen · O. C. Boerman · M. Gotthardt
Department of Radiology and Nuclear Medicine, Radboud university medical center, PO Box 9101, 6500 HB Nijmegen, The Netherlands
e-mail: maarten.brom@radboudumc.nl

T. Bouckenooghe · D. L. Eizirik
Laboratory of Experimental Medicine, Université Libre de Bruxelles (ULB), Brussels, Belgium

P. Rijken
Department of Radiation Oncology, Radboud university medical center, Nijmegen, the Netherlands

B. J. Göke
Department of Internal Medicine II, Ludwig-Maximilians University, Munich, Germany

M. de Jong
Department of Nuclear Medicine, Erasmus Medical Center, Rotterdam, the Netherlands

M. Béhé
Division of Nuclear Medicine and PET Center, University Hospital of Freiburg, Freiburg, Germany

T. Lahoutte
In Vivo Cellular and Molecular Imaging Laboratory, Vrije Universiteit Brussel, Brussels, Belgium

C. J. Tack
Department of Internal Medicine, Radboud university medical center, Nijmegen, the Netherlands

Present address:
T. Bouckenooghe
Cell Biology Research Unit, Life Science Institute, Catholic University of Louvain, Louvain-la-Neuve, Belgium

Present address:
M. Béhé
Center for Radiopharmaceutical Science ETH-PSI-USZ, Paul Scherrer Institute, Villigen, Switzerland

diabetes and five healthy individuals. The tracer uptake was determined by quantitative analysis of the SPECT images.
Results In rats, ^{111}In-labelled exendin specifically targets the beta cells and pancreatic uptake is highly correlated with BCM. In humans, the pancreas was visible in SPECT images and the pancreatic uptake showed high interindividual variation with a substantially lower uptake in patients with type 1 diabetes.
Conclusions/interpretation These studies indicate that ^{111}In-labelled exendin may be suitable for non-invasive quantification of BCM.
Trial registration ClinicalTrials.gov NCT01825148, EudraCT: 2012-000619-10

Keywords Beta cell mass · Exendin · Glucagon-like peptide 1 receptor · Single photon emission computed tomography

Abbreviations

%ID/g	Percentage of injected dose per gram of tissue
Ahx	Aminohexanoic acid
BCM	Beta cell mass
CT	Computed tomography
DTPA	Diethylene triamine pentaacetic acid
[^{18}F]FP-(+)-DTBZ	[^{18}F]Fluoropropyl-dihydrotetrabenazine
GAPDH	Glyceraldehyde-3-phosphate dehydrogenase
GLP-1R	Glucagon-like peptide 1 receptor
mAb	Monoclonal antibody
PET	Positron emission computed tomography
p.i.	Post injection
SPECT	Single photon emission computed tomography
VMAT2	Vesicular monoamine transporter 2
VOI	Volume of interest

Introduction

Diabetes mellitus is characterised by chronically elevated blood glucose levels. In type 1 diabetes, autoimmune destruction of pancreatic beta cells leads to absolute deficiency of insulin secretion with subsequent hyperglycaemia [1]. It is commonly assumed that type 1 diabetes becomes clinically apparent when the remaining beta cell mass (BCM) has decreased to 5–20% [2, 3]. Recent studies, however, suggest that patients with type 1 diabetes may still have a large amount of remaining beta cells [4]; in some patients loss of BCM was less than 50% [5]. Moreover, some patients newly diagnosed with type 1 diabetes who underwent autologous non-myeloablative haematopoietic stem cell transplantation became insulin-independent for several months, suggesting restored function of existing beta cells [6]. In type 2 diabetes, failure of beta cells to adapt to the increased insulin demand, posed by insulin resistance in target tissues, leads to impaired glucose homeostasis [1, 7–10]. BCM changes during the development and course of type 2 diabetes [11], but this process is neither well understood nor well characterised [9]. Moreover, it also appears that BCM and beta cell function do not always correlate over the course of disease [9, 12]. To date, no reliable method exists to measure BCM in humans in vivo and most information has been obtained from autopsy studies of diabetic patients [9] and healthy individuals. Autopsies, however, cannot show the dynamics of BCM at onset and progression of the disease. Therefore, a non-invasive imaging method to quantify BCM in vivo would allow us to gain better insight into the pathophysiology of diabetes during the progression of the disease.

MRI and computed tomography (CT) offer the highest resolution of currently available clinical imaging technology, but neither resolution nor contrast suffices to visualise single pancreatic islets in humans in vivo. Alternative nuclear medicine imaging modalities, such as single photon emission computed tomography (SPECT) or positron emission tomography (PET), offer a very high sensitivity, which may be sufficient for the detection of the relatively low number of pancreatic islet cells by using a highly beta cell-specific radiolabelled tracer molecule. A potential target for measurement of the BCM is the glucagon-like peptide 1 receptor (GLP-1R) as it is abundantly expressed in rat, mouse and human pancreatic beta cells but not in α, δ and pp cells [13, 14]. Exendin is a stable agonist of the GLP-1R and it has been used for in vivo targeting of the GLP-1R after labelling with various radionuclides [15–19]. Exendin labelled with indium-111 could be used to determine the BCM in vivo by SPECT.

To test this hypothesis, we first explored biodistribution and specificity of the ^{111}In-labelled exendin tracer in a rat model of alloxan-induced beta cell loss and subsequently in five patients with type 1 diabetes and five healthy individuals.

Methods

Peptides and radiolabelling for studies in rats [Lys^{40}(DTPA)]exendin-3 and [Lys^{40}]exendin-3 were purchased from Peptides Specialty Laboratories (Heidelberg, Germany). Diethylene triamine pentaacetic acid (DTPA) was conjugated to the ε-amino group of the lysine (K40) and the C-terminal carboxyl group was amidated [15]. Indium-111 labelling and quality control was performed as previously described [15]. ^{111}In-labelled exendin was injected into rats without further purification.

SPECT and biodistribution in diabetic rats To determine the correlation of the uptake of ^{111}In-labelled exendin-3 and the BCM, 6- to 8-week-old female Brown Norway rats (Harlan, Horst, the Netherlands) were injected with various concentrations of alloxan monohydrate (Sigma, St Louis, MO, USA): 15, 30, 45 or 60 mg/kg body weight (n=4 per group; see electronic supplementary material [ESM] Methods for further details). Blood glucose concentrations were determined using a glucose meter (Accu-Chek Sensor; Roche Diagnostics, Almere, the Netherlands) 1 week after injection of alloxan. One week after the injection of alloxan, when hyperglycaemia was confirmed, rats received 15 MBq ^{111}In-labelled exendin-3 intravenously; five control rats were co-injected with an excess of unlabelled exendin-3 (25 μg). One hour post injection (p.i.), SPECT/CT scans were acquired using a dedicated small-animal SPECT/CT scanner (NanoSPECT/CT; Bioscan, Paris, France). After SPECT imaging, the pancreas and other relevant tissues were dissected, weighed and counted in a well-type γ-counter (Wallac 1480-Wizard; Perkin-Elmer, Boston, MA, USA). Pancreases of one rat per group were harvested and snap-frozen in isopentane on dry ice for autoradiography. Cryosections (10 μm) were exposed to an imaging plate (Fuji Film BAS-SR 2025; Raytest, Straubenhardt, Germany) for 72 h. Images were acquired with a radioluminography laser imager (Fuji Film BAS 1800 II system; Raytest) and analysed with Aida Image Analyzer software (Raytest). The pancreases of the remaining rats were fixed in formalin and embedded in paraffin for the determination of the BCM as described below.

Pancreatic BCM was plotted against the pancreatic uptake determined by ex vivo counting.

^{111}In-labelled exendin-3 uptake was quantified using Inveon Research Workplace (Preclinical Solutions, Siemens Medical Solutions USA, Knoxville, TN, USA). See ESM Methods for further details.

SPECT of dissected tissues Brown Norway rats were injected intravenously with 60 mg/kg alloxan monohydrate as described above. When hyperglycaemia was confirmed, diabetic (n=4) and healthy (n=4) rats were injected with 15 MBq ^{111}In-labelled exendin-3. Two control rats were co-injected with an excess of unlabelled exendin-3 (25 μg/rat). Rats were killed 1 h after injection of the radiolabelled exendin and the pancreas, gastrointestinal tract, liver and spleen were dissected and fixed in 4% formalin. SPECT images of the dissected pancreases, along with the gastrointestinal tract, liver and spleen, were acquired on a dedicated small-animal SPECT scanner (U-SPECT-II; MILabs, Utrecht, the Netherlands).

Determination of the BCM Five sections (4 μm) of paraffin-embedded pancreases, 100 μm apart from each other, were stained with an anti-insulin antibody (4 μg/ml in PBS containing 1% BSA w/v) (sc 9168; Santa Cruz Biotechnology, Santa Cruz, CA, USA) as previously described [20].

The surface of the beta cells in the sections was estimated by drawing regions of interest around insulin-stained tissue and total pancreatic tissue on images of the pancreatic section captured using a digital image processing system for bright field microscopy [21] (400 × magnification). The total pancreatic pixel area was determined by automated image thresholding [22] of the hematoxylin-stained pancreatic tissue. The total insulin-positive pixel area was determined by drawing regions of interest over the insulin-positive tissue and the insulin-positive fraction was calculated by dividing the insulin-positive pixel area by the total pancreatic pixel area [23]. The BCM was calculated by multiplying the insulin-positive fraction by the total pancreatic weight.

Microautoradiography One Brown Norway rat was injected intravenously three times with 15 MBq ^{111}In-labelled exendin-3 at intervals of 1 h and the pancreas was harvested 1 h after the last injection. The pancreas was fixed in formalin, embedded in paraffin and 4 μm sections were prepared. The sections were deparaffinised and covered with a homogeneous layer of hypercoat emulsion (Amersham LM-1; GE Healthcare, Little Chalfont, UK) by dipping the slides in the emulsion at 42°C in the dark. After incubation in the dark for 1 week the sections were developed for 4 min in a 6% black and white developer (Agfa studional liquid; Agfa, Leverkusen, Germany). The sections were rinsed in water for 20 s and fixed in 24% (wt/vol.) solution of sodium thiosulphate for 4 min. The sections were rinsed with water, stained with hematoxylin for 30 s, rinsed with water for 10 min, dehydrated and the slide was mounted with mounting fluid. Consecutive sections were stained with an anti-insulin monoclonal antibody as described above for co-localisation.

mRNA extraction and real-time PCR Poly(A)+ mRNA was isolated from rat tissues using the Dynabeads mRNA DIRECT kit (Invitrogen, Merelbeke, Belgium), and reverse transcribed as previously described [24]. Human cDNA was from Gentaur (Brussels, Belgium). The real-time PCR amplification reaction was performed as described [25], using iQ SyBR Green Supermix on iCycler MyiQ Single Color (Bio-Rad, Hercules, CA, USA), and compared with a standard curve [26]. Expression values were corrected for the housekeeping gene glyceraldehyde-3-phosphate dehydrogenase (GAPDH). The primers used are summarised in Table 1.

Preparation and labelling of ^{111}In-labelled exendin for human use [Lys^{40}(Ahx-DTPA)]exendin-4 (where Ahx represents aminohexanoic acid) for clinical use was produced (piCHEM, Graz, Austria), dissolved and portioned according to GMP standards to a final concentration of 2 μg/ml in 1 mol/l HEPES

Table 1 Primers used for quantitative PCR

1	2 Sequence (5′–3′)	3 Base pairs
Rat *Gapdh*		118
Forward	AGTTCAACGGCACAGTCAAG	
Reverse	TACTCAGCACCAGCATCACC	
Rat *Glp1r*		108
Forward	GCTGCCCTCAAGTGGATGTA	
Reverse	ATGAGCAGGAACACCAGTCG	
Human *GAPDH*		136
Forward	AGTTCAACGGCACAGTCAAG	
Reverse	TACTCAGCACCAGCATCACC	
Human *GLP1R*		114
Forward	TCCTCCTCGGCTTCAGACACCTGCA	
Reverse	CCACTTCAGGGCTGCGTCCTTGATG	

(pH 5.5) containing 0.1% Tween 80. The vials were stored at −20°C. Radiolabelling was performed by adding exendin to the vial containing $^{111}InCl_3$ to a final concentration of 150 MBq $^{111}InCl_3$ per μg [Lys^{40}(Ahx-DTPA)]exendin-4. After incubation at room temperature for 30 min 0.25 ml EDTA (3.75 mg/ml) was added and quality control was performed as described above. Finally, the volume was adjusted to 5 ml with 0.9% NaCl before administration.

Type 1 diabetic patients and healthy controls Five patients with type 1 diabetes, who met the inclusion criteria listed in Table 2, were included in this study. Only patients with type 1 diabetes without insulin production, as confirmed by undetectable non-stimulated and stimulated C-peptide (<0.03 nmol/l), were included. To create two comparable groups, healthy controls matched for BMI (maximum difference 2 kg/m^2), age (maximum difference 10 year) and sex were selected for participation. Only healthy controls with HbA_{1c} <7% (53 mmol/mol) and normal glucose tolerance, assessed by an OGTT, were included.

Table 2 Inclusion criteria

Criterion	Range
BMI, kg/m^2	18.5–27.0
Age, years	21–60
No previous treatment with exenatide or dipeptidyl-peptidase IV inhibitors	
Creatinine clearance (MDRD), ml/min	≥40
Type 1 diabetic patients	
No stimulated insulin production: C-peptide, nmol/l	Not measurable (< 0.03)
Time since diagnosis of type 1 diabetes, years	> 5
Healthy controls	
HbA_{1c}, %	<7
HbA_{1c}, mmol/mol	53
Normal glucose tolerance: blood glucose 2 h after OGTT, mmol/l	<7.8

MDRD, modification of diet in renal diseases

An overview of the participants included in the study is given in Table 3. Written informed consent was obtained from all study participants in accordance with provisions of the Declaration of Helsinki, and the study was approved by the Institutional Ethics Review Board of the Radboud university medical center.

Administration of radiotracer After participants had fasted for at least 4 h, 150 MBq ^{111}In-labelled exendin, corresponding to a peptide dose of 1 μg exendin, was injected as a slow bolus over 5 min.

Image acquisition At 4 h, 24 h and 48 h after ^{111}In-labelled exendin administration, SPECT was acquired using an integrated SPECT/CT scanner (Symbia T16; Siemens Healthcare, Molecular Imaging, Hoffman Estates, IL, USA) and CT images were acquired 24 h post injection. See ESM Methods for further details.

SPECT reconstruction SPECT images were reconstructed with Hermes Hybrid Recon software (Version 1.0C, Hermes Medical Solutions, Stockholm, Sweden), in six iterations, 16 subsets and a matrix size of 128×128 (corresponding with an isotropic voxel size of 4.7952 mm). CT-based attenuation correction and Monte Carlo-based scatter correction was performed. Post-reconstruction filtering was applied with a 1.0 cm Gauss filter.

Quantification of SPECT images Image quantification was performed with Inveon Research Workplace software (Version 4.1, Siemens, Munich, Germany). The CT image was used for delineation of the pancreas. Within the pancreas two spherical volumes of interest (VOIs), one in the head and one in the corpus, were used for determination of the pancreatic uptake. See ESM Methods for further details.

Statistical analysis All mean values are expressed as mean ± SD. Statistical analysis was performed using the unpaired two-tailed *t* test using GraphPad Prism (version 4, GraphPad Software, San Diego, CA, USA). The level of significance was set at $p<0.05$.

Correlation between the BCM and pancreatic uptake was determined by the Pearson correlation coefficient (*r*) using two-tailed analysis of variance with GraphPad Prism (version 4). The level of significance was set at $p<0.05$.

Table 3 Overview of included participants

Participant	Age, years	BMI, kg/m^2	Sex	Type 1 diabetes duration, years	HbA_{1c}, % (mmol/mol)	CT-based pancreas volume, cm^3	Uptake in the whole pancreas, counts
Patients with type 1 diabetes							
D1	50	26.1	M	30	7.3 (56)	51.6	239
D2	25	21.3	F	13	8.4 (68)	63.6	1,445
D3	47	23.6	M	27	6.7 (50)	45.9	185
D4	54	21.9	F	33	7.4 (57)	20.7	92
D5	41	25.2	F	27	6.7 (50)	72.1	612
Healthy controls							
H1	54	24.3	M		5.6 (38)	88.8	263
H2	24	19.8	F		5.6 (38)	72.7	1,821
H3	40	23.9	M		5.3 (34)	106.6	1,844
H4	54	22.4	F		5.4 (35)	73.8	899
H5	43	24.1	F		5.4 (35)	83.1	1,577

M, male; F, female

Results

Radiolabelling A specific activity of 700 GBq/μmol for ^{111}In-labelled exendin-3 was obtained with a radiochemical purity exceeding 95%.

Biodistribution studies Biodistribution in Brown Norway rats 1 h p.i. showed tracer uptake in various organs (Fig. 1a). ^{111}In-labelled exendin accumulated in the pancreas to a concentration of 0.29±0.04% (expressed as the percentage of injected dose per gram of tissue [%ID/g]). Co-injection of excess unlabelled exendin resulted in a marked decrease in pancreatic uptake (0.04±0.01%ID/g), indicating that the uptake of the tracer is GLP-1R mediated, which also holds for the uptake in the stomach and the duodenum (0.33±0.03%ID/g and 0.44±0.08%ID/g, respectively). In addition, very high specific uptake was observed in the lungs, known to express high levels of GLP-1R in rodents: 13.45±2.50%ID/g. Kidney uptake was also very high (29.2±2.3%ID/g) and was not blocked by an excess of unlabelled exendin. Severely diabetic rats showed an 80% reduction in pancreatic uptake (0.06±0.01%ID/g).

The uptake of ^{111}In-exendin in the pancreas was plotted against the BCM (Fig. 1f) showing a good correlation between these two variables (Pearson r=0.89).

Ex vivo autoradiography Autoradiography of pancreatic sections of alloxan-treated and control rats demonstrated that the tracer specifically accumulated in the islets of Langerhans: high concentrations of ^{111}In-exendin were observed in hotspots throughout the pancreatic section in control rats, representing the islets of Langerhans (Fig. 1b, c). The uptake was GLP-1R-mediated since it could be blocked by an excess of unlabelled exendin (Fig. 1b). Very low uptake of the tracer in the exocrine pancreas was observed (Fig. 1b, c). When rats were treated with alloxan, the tracer uptake in the islets was reduced (Fig. 1b).

Immunohistochemical staining of the pancreatic sections with an anti-insulin monoclonal antibody (mAb) showed co-localisation of the stained islets and the hotspots observed in autoradiography (Fig. 1c), demonstrating specific accumulation in the islets. Microautoradiography (Fig. 1d) also showed islet-specific tracer uptake, which was co-localised with immunohistochemical staining of a consecutive pancreas section with an anti-insulin mAb (Fig. 1e).

SPECT of dissected tissues To visualise the uptake of ^{111}In-labelled exendin in the abdominal organs, SPECT scans of dissected organs in the peritoneal cavity of alloxan-treated and control Brown Norway rats were acquired (Fig. 2). The uptake of ^{111}In-labelled exendin in the pancreases of untreated Brown Norway rats was clearly visualised, whereas the pancreases of alloxan-treated rats, as well as those from rats co-injected with an excess unlabelled exendin, were barely visible by ex vivo SPECT (Fig. 2a–c). The resolution of the SPECT scanner was 600 μm, so individual islets of Langerhans could not be visualised (Fig. 2d). Blocking with an excess of unlabelled exendin resulted in a very low pancreatic uptake similar to the uptake in severely diabetic rats. Figure 2e, f shows the ex vivo SPECT images of the dissected gastrointestinal tract, spleen, liver and pancreas after injection of ^{111}In-labelled exendin. A strong signal was observed in the pancreas, whereas other abdominal organs showed only low uptake except for the proximal part of the duodenum and the distal part of the stomach, which showed relatively high uptake.

SPECT and quantitative analysis of SPECT images of diabetic rats The SPECT images of dissected tissues enabled accurate

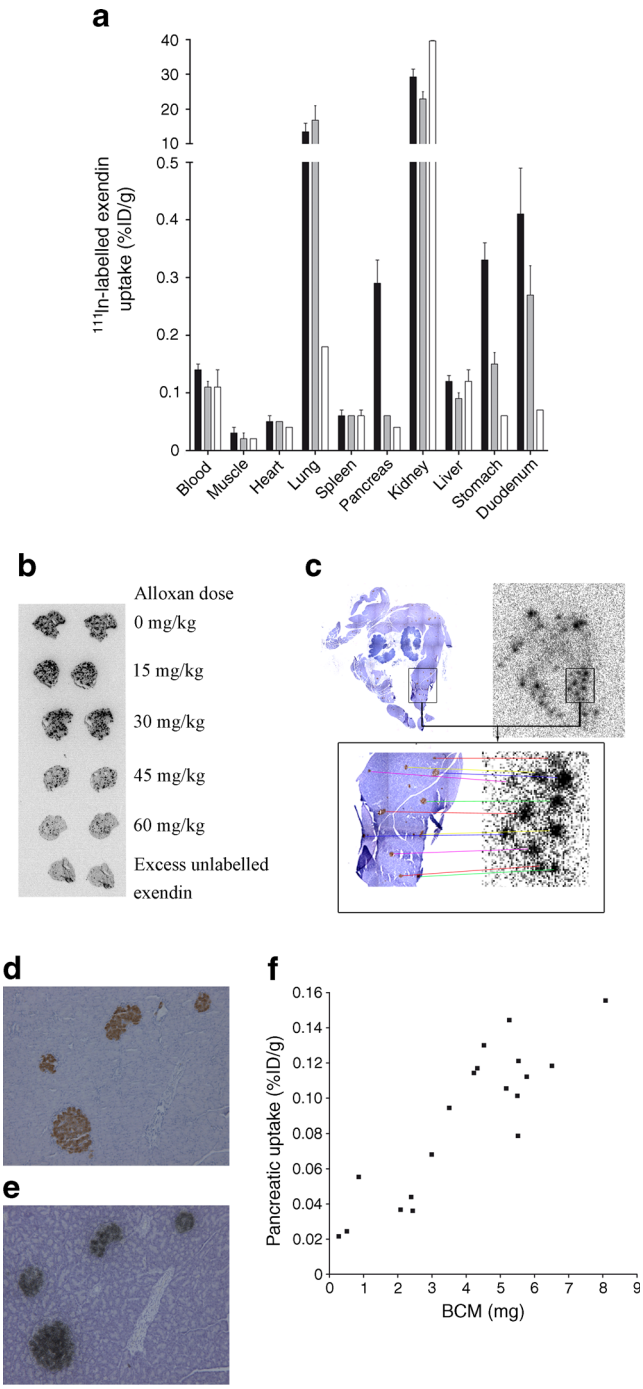

◀ **Fig. 1** (**a**) Biodistribution of ^{111}In-labelled exendin in control (n=4) and alloxan-treated (60 mg/kg) (n=4) Brown Norway rats (expressed as % injected dose/g tissue [%ID/g]), blocking by co-injection of a 250-fold molar excess of unlabelled exendin (n=2). Organs were dissected 1 h p.i. Black bars, control rats; grey bars, alloxan-treated rats; white bars, excess unlabelled exendin. (**b**) Macroautoradiography of consecutive pancreatic sections (10 μm) of control and alloxan (15–60 mg/kg)-treated Brown Norway rats (15 MBq ^{111}In-labelled exendin [0.1 μg], dissection 1 h p.i.). (**c**) A section (4 μm) of pancreatic tissue (embedded in paraffin) of a control rat (magnification ×4) was counterstained with an anti-insulin mAb (brown) after exposure to the imaging plate. The immunohistochemically stained islets are connected with the representative radiosignal with arrows on enlarged section. (**d**, **e**) Microautoradiography (**d**) shows exclusive uptake in the islets and excellent correlation with immunohistochemical staining (**e**) with anti-insulin mAb (magnification ×100). (**f**) Correlation between the uptake of ^{111}In-labelled exendin in rats injected with alloxan (0, 15, 30, 45 and 60 mg/kg) and BCM. The BCM was determined by morphometric analysis after immunohistochemical staining with an anti-insulin antibody on the x-axis. The correlation as determined by Pearson test is r=0.89

interpretation of the SPECT images of Brown Norway rats (Fig. 2g). After injection of ^{111}In-labelled exendin into healthy Brown Norway rats, uptake in the pancreas was visible in SPECT scans.

In diabetic rats there was negligible uptake in the pancreatic region and lower uptake was observed in rats with reduced BCM. Besides high uptake in the pancreas, uptake was also observed in the kidneys and lungs. Moreover, SPECT images after injection of ^{99m}Tc-labelled demobesin 3, specifically accumulating in the pancreas [27], correlated with the pancreatic uptake of ^{111}In-labelled exendin (ESM Fig. 1), confirming that the VOI used for quantification of BCM is indeed located in the pancreas. As previously described, the pancreas is the organ with the highest uptake of the bombesin analogue in the peritoneal cavity of rats [28], due to efficient binding to the gastrin-releasing peptide receptor, which is abundantly expressed in the pancreas [29, 30]. Removal of both kidneys enabled more accurate visualisation of the pancreas, showing exact co-localisation of ^{99m}Tc-labelled demobesin and ^{111}In-labelled exendin as an additional proof that the VOI used for quantification contained the pancreas (ESM Fig. 1). The tracer uptake of ^{111}In-labelled exendin, as determined by quantitative analysis of the SPECT images, correlates linearly with the BCM determined by morphometric analysis (Fig. 2h, Pearson r=0.83).

Quantitative PCR To determine the *Glp1r* mRNA expression in human and rat tissues, quantitative RT-PCR was performed. In rats, a 13-fold higher *Glp1r* mRNA expression was found in the endocrine pancreas compared with the exocrine pancreas (Fig. 3a). The quantitative PCR on human tissues (Fig. 3b) showed high expression of *GLP1R* mRNA in the endocrine pancreas and very low expression in the exocrine pancreas (endocrine–exocrine ratio of 47). These results indicate that the GLP-1R expression profile is even more favourable in humans than in rats.

SPECT/CT in humans We explored the feasibility of the technology to determine the BCM in vivo in patients with type 1 diabetes (n=5) and matching healthy controls (n=5). ^{111}In-labelled exendin uptake was clearly visible in the human pancreas (Fig. 4a, b). The pancreatic uptake of ^{111}In-labelled exendin was clearly decreased in patients with type 1 diabetes (Fig. 4c), with marked differences between patients with type 1

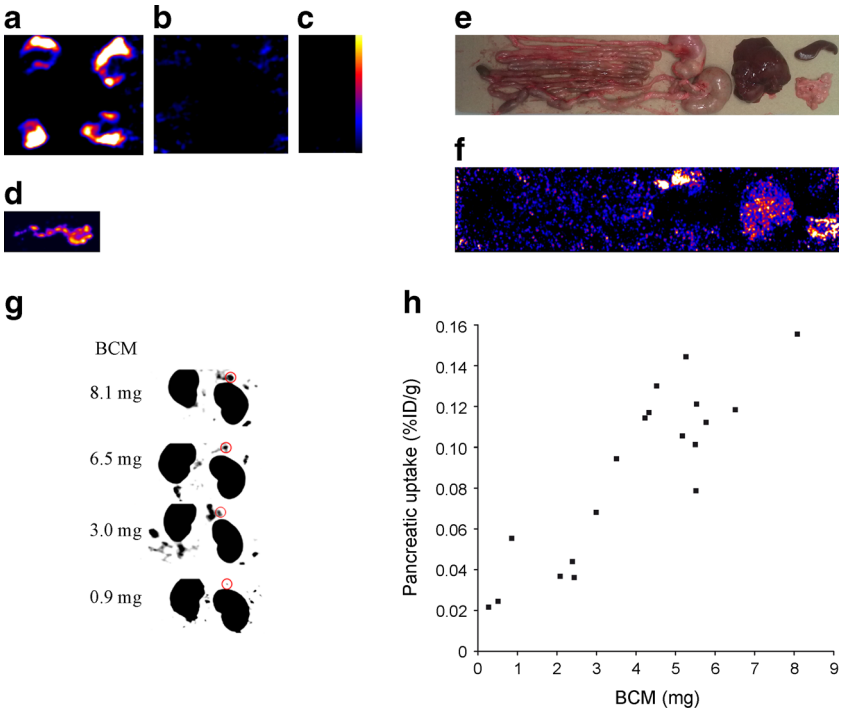

Fig. 2 (**a**–**c**) Ex vivo SPECT images of pancreases from control (**a**) and alloxan-treated Brown Norway rats (**b**); blocking (**c**) was performed with an excess of unlabelled exendin (25 μg) in two rats. (**d**–**f**) Ex vivo SPECT images of the gastrointestinal tract of Brown Norway rats (**e**, **f**) and a high-resolution SPECT scan of a pancreas (**d**). (**g**) ^{111}In-labelled exendin SPECT scans of Brown Norway rats with different BCMs (acquired 1 h p.i.). Red circles indicate the pancreas. (**h**) Correlation between ^{111}In-labelled exendin uptake determined by quantitative analysis of SPECT scans and BCM (BCM was determined by morphometric analysis after immunohistochemical staining with anti-insulin antibody). The correlation as determined by Pearson test is r=0.83

diabetes and healthy controls. Nevertheless, there was some overlap in pancreatic uptake of ^{111}In-labelled exendin between the groups. There was no significant difference in pancreatic uptake of ^{111}In-labelled exendin at 4, 24 or 48 h after injection (Fig. 4d).

Discussion

In this study, we systematically characterised ^{111}In-labelled exendin in rats for the non-invasive determination of pancreatic BCM by SPECT. The key findings of these studies are: (1) There is specific GLP-1R-mediated uptake of ^{111}In-labelled exendin in the pancreas; (2) ^{111}In-labelled exendin localises specifically in the islets of Langerhans in rats; (3) the pancreatic uptake of ^{111}In-labelled exendin determined by ex vivo counting correlates linearly with BCM (Pearson r=0.89); (4) rats treated with high doses of alloxan, representing a controlled model of severe beta cell loss, showed an 80% reduction of tracer uptake in the pancreas indicating that even small differences in BCM can be detected; (5) the pancreatic tracer uptake decreased with decreasing

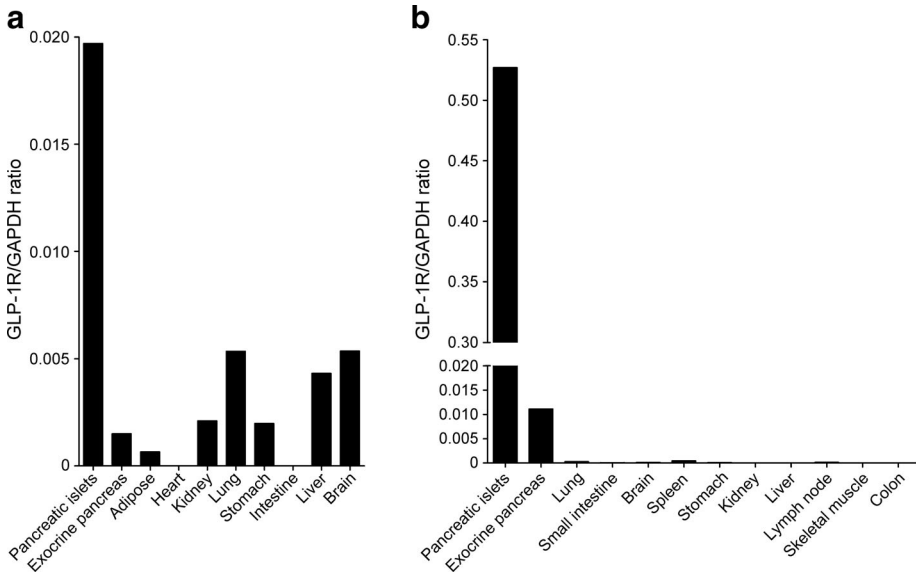

Fig. 3 Quantitative PCR for *Glp1r*/*GLP1R* in rat (**a**) and human (**b**) tissue samples, including endocrine and exocrine pancreas. Results are representative of three similar experiments

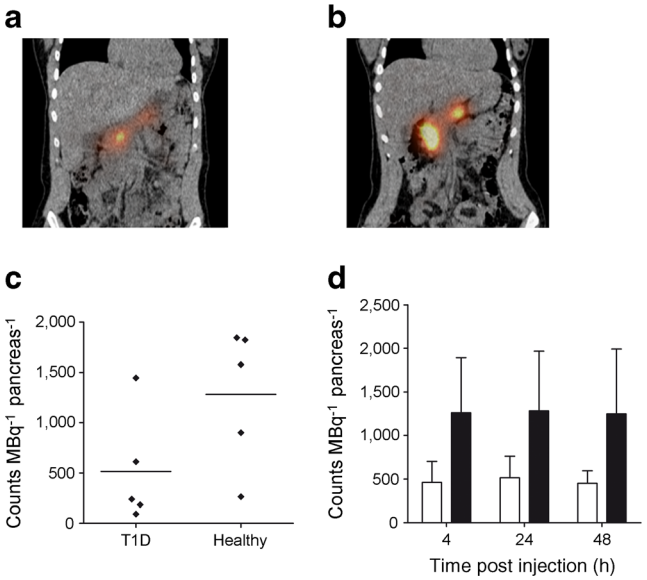

Fig. 4 In vivo SPECT/CT images of the abdomen in humans, acquired 24 h after injection of ^{111}In-labelled exendin. (**a**, **b**) Coronal cross-sections of a patient with type 1 diabetes (**a**) and a healthy individual (**b**) both show high uptake in the pancreas. (**c**) Pancreatic uptake of ^{111}In-labelled exendin quantified in SPECT images of five patients with type 1 diabetes (T1D) and five healthy individuals. Uptake was corrected for administered activity (142–153 MBq) and time after injection (23.2–24.7 h), resulting in pancreas uptake in total counts. The lines indicate the mean uptake per group. (**d**) Mean and SD of the activity in the pancreas per group, per scan moment (4 h, 24 h and 48 h post injection). White bars, patients with type 1 diabetes; black bars, healthy individuals

BCM and only minimal uptake was observed in rats treated with high doses of alloxan; (6) most importantly, the uptake of tracer by the pancreas could be visualised by in vivo SPECT and quantitative analysis of the SPECT data correlated with the BCM in a linear manner (Pearson r=0.83).

We have previously shown that the peptide dose is a critical factor that determines the uptake of ^{111}In-labelled exendin in GLP-1R-positive tissues [15]. It should be noted that the specific and high uptake of the tracer in the pancreas in this rat model is only observed at peptide doses not exceeding 0.1 μg per rat; at higher doses the GLP-1Rs in the pancreas are saturated as shown in the in vivo blocking experiments. Therefore, a tracer with a very high specific activity is required for SPECT [15]. We have therefore improved the specific activity of ^{111}In-labelled exendin up to 700 MBq/nmol, which allows administration of sufficient radioactivity for SPECT without exceeding the tracer dose of 0.1 μg/rat.

Previous preclinical studies with exendin labelled with ^{18}F or ^{64}Cu have demonstrated their ability to visualise transplanted islets and subcutaneous tumours in rodents [18, 19]. For the GLP-1R antagonist exendin-(9–39) labelled with ^{18}F, however, no correlation between uptake and pancreatic BCM could be demonstrated in a rat model [16]. This is probably due to the fact that the antagonist exendin-(9–39) is not suitable for in vivo targeting of the GLP-1R [31], indicating that agonistic activity is required for successful visualisation of beta cells in vivo. Importantly, Reiner et al have recently demonstrated the in vivo targeting of beta cells with a fluorescent labelled exendin-4 analogue [32].

Previous studies suggested that GLP-1R expression is detected in the exocrine pancreas by in vitro autoradiography with ^{125}I-GLP-1 and immunohistochemistry on human pancreatic sections [13, 33]. Our ex vivo autoradiographic analysis showed scattered focal hotspots throughout the pancreas that were co-localised with the islets in immunohistochemical staining with only low background activity in the exocrine pancreas. This focal uptake decreased with alloxan-induced loss of BCM and was almost completely absent in severely diabetic rats. The results of our ex vivo autoradiography are in line with the quantitative PCR analysis on rat tissues: high GLP-1R expression was observed in the endocrine pancreas, while low expression was apparent in the exocrine pancreas. The differences observed between our results and the previously published data [13, 33] may be explained by differences between binding characteristics of ^{125}I-labelled glucagon-like peptide 1 and GLP-1R antibodies in an in vitro assay as compared with the binding characteristics of ^{111}In-labelled exendin in vivo. Of note, in vivo ^{111}In-labelled exendin also shows internalisation and metabolic trapping [34], which makes this technology highly sensitive and specific for the detection of GLP-1R-positive tissues. In addition, artefacts potentially occurring in vitro leading to non-specific binding are avoided.

It was previously reported that the GLP-1R expression is decreased in pancreatic islets in hyperglycaemic rats after near total pancreatectomy or constant glucose infusion [35], as determined by immunohistochemical staining and quantitative PCR. Our data show a strong correlation of tracer uptake and BCM under euglycaemic as well as severe hyperglycaemic conditions. This observation argues against changes in GLP-1R expression having a significant influence on ^{111}In-labelled exendin uptake. In addition, quantitative RT-PCR showed that the endocrine–exocrine GLP-1R expression ratio is even higher in humans than in rats (endocrine–exocrine ratio 47 in humans vs 13 in rats). Of note, we cannot exclude some contamination of the exocrine pancreas with insulin-producing cells, so that the actual endocrine–exocrine ratio of *GLP1R* mRNA expression may be even higher.

After these promising preclinical findings, we explored the feasibility of this technology to determine the BCM in vivo in patients with type 1 diabetes (n=5) and matching healthy controls (n=5). The pancreatic uptake of ^{111}In-labelled exendin showed considerable interindividual variation, in line with variations in BCM as reported in the literature [12, 36]. The pancreatic uptake of ^{111}In-labelled exendin was clearly decreased in patients with type 1 diabetes, with marked

differences between diabetic patients and healthy individuals. To date, no other radiotracer tested for BCM determination has shown such large maximum differences between healthy individuals and patients with type 1 diabetes, nor has such a high interindividual variability of the uptake been reported previously [37–44]. A recent study in healthy individuals and patients with type 1 diabetes, involving PET after injection of [^{18}F]fluoropropyl-dihydrotetrabenazine ([^{18}F]FP-(+)-DTBZ), showed a maximum difference in pancreatic uptake of <40% [45]. The difference in binding potential between patients with type 1 diabetes and healthy individuals was not greater than 50% [45]. Moreover, a recent publication showed that expression of vesicular monoamine transporter 2 (VMAT2) in pancreatic polypeptide cells causes overestimation of the BCM in type 1 diabetes, as determined by PET measurements [46]. In this study, the authors demonstrated that PP cells express VMAT2 and this contributes to the total pancreatic uptake of [^{18}F]FP-(+)-DTBZ. These data are in line with the reduction in pancreatic uptake of [^{18}F]FP-(+)-DTBZ by less than 40% in patients with type 1 diabetes. The markedly higher difference in pancreatic uptake of ^{111}In-labelled exendin between healthy individuals and patients with type 1 diabetes points towards a considerably higher specificity of ^{111}In-labelled exendin for beta cells.

Of note, the dynamic scanning protocol previously described, including arterial blood sampling, makes this a laborious procedure. Our SPECT protocol with ^{111}In-labelled exendin is a much simpler method that requires a single injection of the radiotracer followed by single time point static SPECT acquisition and subsequent quantitative analysis of the images. In addition, the method can be used in every hospital equipped with a gamma camera, does not require a cyclotron and the labelled compound can easily be distributed ready to use for clinical studies.

In summary, we here demonstrate in a preclinical imaging model of beta cell loss that the uptake of ^{111}In-exendin, as determined by in vivo imaging, is specific for the beta cells and shows a direct correlation with BCM. In humans, we observed considerable interindividual differences in pancreatic tracer uptake (in line with available autopsy data) and a marked reduction in pancreatic uptake in patients with type 1 diabetes. To the best of our knowledge, so far there is no comparable preclinical evidence for any other radiotracer tested for in vivo imaging of BCM with respect to beta cell specificity and correlation of uptake to actual BCM. Of note, clinical imaging does not require complicated dynamic scanning techniques or calculation of binding capacity, making it feasible for efficient use in large clinical trials [19]. Therefore, our data indicate that this technology could indeed be the first to enable non-invasive determination of BCM in humans, offering great potential to better elucidate the pathophysiology of the different types and stages of diabetes.

Acknowledgements We thank T. Maina and B. Nock (National Centre for Scientific Research 'Demokritos', Athens, Greece) for kindly providing demobesin-3 and M. Melis, J. de Swart and E. de Blois (Department of Nuclear Medicine, Erasmus Medical Centre, Rotterdam, the Netherlands) for technical support of the SPECT experiments. H. de Wit (Department of Internal Medicine, Radboud university medical center, Nijmegen, the Netherlands) assisted in the recruitment of patients. We acknowledge W. Grootjans (Department of Radiology and Nuclear Medicine, Radboud university medical center, Nijmegen, the Netherlands) for technical assistance in image analysis of the patient data.

Funding Our work was supported by NIH grant 1R01 AG 030328-01 and the European Community's Seventh Framework Programme (FP7/2007-2013) project BetaImage, under grant agreement No. 222980.

Duality of interest The authors declare that there is no duality of interest associated with this manuscript.

Contribution statement MB and WW designed the experiments and acquired, analysed and interpreted the data and drafted and critically revised the manuscript. PR, LJ, CF, KA, TL, MJ, OCB, MG and TB provided a substantial contribution to the conception and design, acquisition of data, or analysis and interpretation of data. BJG, MdJ, DLE, MBe, WO and CJT contributed to analysis and interpretation of the data. LJ, CF, KA, CJT, MBé, MdJ, BJG, DLE, WJG, TB, PR, TL and MJ critically revised the manuscript for important intellectual content. OCB and MG provided a substantial contribution to the conception and design, acquisition of data, or analysis and interpretation of data and critically revised the manuscript for important intellectual content. All authors approved the final version of the manuscript. MG is responsible for the integrity of the work as a whole.

References

1. American Diabetes Association (2006) Diagnosis and classification of diabetes mellitus. Diabetes Care 29(Suppl 1):S43–S48
2. Lohr M, Kloppel G (1987) Residual insulin positivity and pancreatic atrophy in relation to duration of chronic type 1 (insulin-dependent) diabetes mellitus and microangiopathy. Diabetologia 30:757–762
3. Steele C, Hagopian WA, Gitelman S et al (2004) Insulin secretion in type 1 diabetes. Diabetes 53:426–433
4. Coppieters KT, Dotta F, Amirian N et al (2012) Demonstration of islet-autoreactive CD8 T cells in insulitic lesions from recent onset and long-term type 1 diabetes patients. J Exp Med 209:51–60
5. Klinke DJ 2nd (2008) Extent of beta cell destruction is important but insufficient to predict the onset of type 1 diabetes mellitus. PloS ONE 3:e1374
6. Couri CE, Oliveira MC, Stracieri AB et al (2009) C-peptide levels and insulin independence following autologous nonmyeloablative hematopoietic stem cell transplantation in newly diagnosed type 1 diabetes mellitus. JAMA 301:1573–1579
7. DeFronzo RA (1997) Pathogenesis of type 2 diabetes: metabolic and molecular implications for identifying diabetes genes. Diabetes Rev 5:177–269
8. Taylor SI (1999) Deconstructing type 2 diabetes. Cell 97:9–12
9. Weir GC, Bonner-Weir S (2004) Five stages of evolving beta-cell dysfunction during progression to diabetes. Diabetes 53(Suppl 3): S16–S21
10. Cnop M, Welsh N, Jonas JC, Jorns A, Lenzen S, Eizirik DL (2005) Mechanisms of pancreatic beta-cell death in type 1 and type 2 diabetes: many differences, few similarities. Diabetes 54(Suppl 2): S97–S107

11. Butler AE, Janson J, Bonner-Weir S, Ritzel R, Rizza RA, Butler PC (2003) Beta-cell deficit and increased beta-cell apoptosis in humans with type 2 diabetes. Diabetes 52:102–110
12. Ritzel RA, Butler AE, Rizza RA, Veldhuis JD, Butler PC (2006) Relationship between beta-cell mass and fasting blood glucose concentration in humans. Diabetes Care 29:717–718
13. Korner M, Stockli M, Waser B, Reubi JC (2007) GLP-1 receptor expression in human tumors and human normal tissues: potential for in vivo targeting. J Nucl Med 48:736–743
14. Tornehave D, Kristensen P, Romer J, Knudsen LB, Heller RS (2008) Expression of the GLP-1 receptor in mouse, rat, and human pancreas. J Histochem Cytochem 56:841–851
15. Brom M, Oyen WJ, Joosten L, Gotthardt M, Boerman OC (2010) 68Ga-labelled exendin-3, a new agent for the detection of insulinomas with PET. Eur J Nucl Med Mol Imaging 37:1345–1355
16. Wang Y, Lim K, Normandin M, Zhao X, Cline GW, Ding YS (2012) Synthesis and evaluation of [18F]exendin (9-39) as a potential biomarker to measure pancreatic beta-cell mass. Nucl Med Biol 39:167–176
17. Wild D, Wicki A, Mansi R et al (2010) Exendin-4-based radiopharmaceuticals for glucagonlike peptide-1 receptor PET/CT and SPECT/CT. J Nucl Med 51:1059–1067
18. Wu Z, Liu S, Hassink M et al (2013) Development and evaluation of 18F-TTCO-Cys40-Exendin-4: a PET probe for imaging transplanted islets. J Nucl Med 54:244–251
19. Wu Z, Todorov I, Li L et al (2011) In vivo imaging of transplanted islets with 64Cu-DO3A-VS-Cys40-Exendin-4 by targeting GLP-1 receptor. Bioconjug Chem 22:1587–1594
20. Heskamp S, van Laarhoven HW, Molkenboer-Kuenen JD et al (2010) ImmunoSPECT and immunoPET of IGF-1R expression with the radiolabeled antibody R1507 in a triple-negative breast cancer model. J Nucl Med 51:1565–1572
21. Rademakers SE, Rijken PF, Peeters WJ et al (2011) Parametric mapping of immunohistochemically stained tissue sections; a method to quantify the colocalization of tumor markers. Cell Oncol (Dordr) 34:119–129
22. Rijken PF, Bernsen HJ, van der Kogel AJ (1995) Application of an image analysis system to the quantitation of tumor perfusion and vascularity in human glioma xenografts. Microvasc Res 50:141–153
23. Garofano A, Czernichow P, Breant B (1998) Beta-cell mass and proliferation following late fetal and early postnatal malnutrition in the rat. Diabetologia 41:1114–1120
24. Chen CM, Behringer RR (2001) Cloning, structure, and expression of the mouse Ovca1 gene. Biochem Biophys Res Commun 286: 1019–1026
25. Cunha DA, Hekerman P, Ladriere L et al (2008) Initiation and execution of lipotoxic ER stress in pancreatic beta-cells. J Cell Sci 121:2308–2318
26. Overbergh L, Valckx D, Waer M, Mathieu C (1999) Quantification of murine cytokine mRNAs using real time quantitative reverse transcriptase PCR. Cytokine 11:305–312
27. Nock BA, Nikolopoulou A, Galanis A et al (2005) Potent bombesin-like peptides for GRP-receptor targeting of tumors with 99mTc: a preclinical study. J Med Chem 48:100–110
28. Maina T, Nock BA, Zhang H et al (2005) Species differences of bombesin analog interactions with GRP-R define the choice of animal models in the development of GRP-R-targeting drugs. J Nucl Med 46: 823–830
29. Jensen RT, Moody T, Pert C, Rivier JE, Gardner JD (1978) Interaction of bombesin and litorin with specific membrane receptors on pancreatic acinar cells. Proc Natl Acad Sci U S A 75:6139–6143
30. Moran TH, Moody TW, Hostetler AM, Robinson PH, Goldrich M, McHugh PR (1988) Distribution of bombesin binding sites in the rat gastrointestinal tract. Peptides 9:643–649
31. Brom M, Joosten L, Oyen WJ, Gotthardt M, Boerman OC (2012) Radiolabelled GLP-1 analogues for in vivo targeting of insulinomas. Contrast Media Mol Imaging 7:160–166
32. Reiner T, Thurber G, Gaglia J et al (2011) Accurate measurement of pancreatic islet β-cell mass using a second-generation fluorescent exendin-4 analog. Proc Natl Acad Sci U S A 108:12815–12820
33. Xu G, Kaneto H, Lopez-Avalos MD, Weir GC, Bonner-Weir S (2006) GLP-1/exendin-4 facilitates beta-cell neogenesis in rat and human pancreatic ducts. Diabetes Res Clin Pract 73:107–110
34. Brom M, Andralojc K, Oyen WJ, Boerman OC, Gotthardt M (2010) Development of radiotracers for the determination of the beta-cell mass in vivo. Curr Pharm Des 16:1561–1567
35. Xu G, Kaneto H, Laybutt DR et al (2007) Downregulation of GLP-1 and GIP receptor expression by hyperglycemia—possible contribution to impaired incretin effects in diabetes. Diabetes 56:1551–1558
36. Rahier J, Guiot Y, Goebbels RM, Sempoux C, Henquin JC (2008) Pancreatic beta-cell mass in European subjects with type 2 diabetes. Diabetes Obes Metab 10(Suppl 4):32–42
37. Moore A, Bonner-Weir S, Weissleder R (2001) Noninvasive in vivo measurement of beta-cell mass in mouse model of diabetes. Diabetes 50:2231–2236
38. Freeby M, Goland R, Ichise M, Maffei A, Leibel R, Harris P (2008) VMAT2 quantitation by PET as a biomarker for beta-cell mass in health and disease. Diabetes Obes Metab 10(Suppl 4):98–108
39. Goland R, Freeby M, Parsey R et al (2009) 11C-dihydrotetrabenazine PET of the pancreas in subjects with long-standing type 1 diabetes and in healthy controls. J Nucl Med 50:382–389
40. de Lonlay P, Simon-Carre A, Ribeiro MJ et al (2006) Congenital hyperinsulinism: pancreatic [18F]fluoro-L-dihydroxyphenylalanine (DOPA) positron emission tomography and immunohistochemistry study of DOPA decarboxylase and insulin secretion. J Clin Endocrinol Metab 91:933–940
41. Hardy OT, Hernandez-Pampaloni M, Saffer JR et al (2007) Diagnosis and localization of focal congenital hyperinsulinism by 18F-fluorodopa PET scan. J Pediatr 150:140–145
42. Otonkoski T, Nanto-Salonen K, Seppanen M et al (2006) Noninvasive diagnosis of focal hyperinsulinism of infancy with [18F]-DOPA positron emission tomography. Diabetes 55:13–18
43. Rubi B, Ljubicic S, Pournourmohammadi S et al (2005) Dopamine D2-like receptors are expressed in pancreatic beta cells and mediate inhibition of insulin secretion. J Biol Chem 280:36824–36832
44. Sweet IR, Cook DL, Lernmark A et al (2004) Systematic screening of potential beta-cell imaging agents. Biochem Biophys Res Commun 314:976–983
45. Normandin MD, Petersen KF, Ding YS et al (2012) In vivo imaging of endogenous pancreatic beta-cell mass in healthy and type 1 diabetic subjects using F-18-fluoropropyl-dihydrotetrabenazine and PET. J Nucl Med 53:908–916
46. Freeby M, Ichise M, Harris PE (2012) Vesicular monoamine transporter, type 2 (VMAT2) expression as it compares to insulin and pancreatic polypeptide in the head, body and tail of the human pancreas. Islets 4:393–397